THE INFLUENCE OF SOME PARAMETERS OF POLYPROPYLENE FILAMENTS ON THEIR RHEOLOGICAL CHARACTERISTICS

(PART I*)

By

L. KÓCZY, I. FÜLÖP and F. GELEJI

Department of Textile Technology and Light Industry, Technical University, Budapest

(Received July 30, 1971)

1. Introduction

The speedy development in the production of man-made fibres in the last 10 years made possible the manufacture of fibres with special properties in the field of various — chemically different — fibre groups. Fibres of new mechanical properties and morphology have been developed which were suitable to meet special demands of textile processing and end-uses. So were developed among others the so-called tufting "yarns" which really are thick continuous filaments texturized in a stuffing chamber. These filaments are being exclusively used for the manufacture of tufted carpets and floor coverings.

In view of this exclusive end-use, mechanical properties of tufting filaments should be developed so that they present an optimal behaviour against the stresses of tufting techniques on the one hand and best performance in a finished product of floor covering, on the other.

For the purpose of tufting "yarns" and filaments, polyamide and polypropylene fibres, respectively, have been used in the first instance. Both show an excellent resistance to abrasion and are therefore well suited for the primary requirements for carpets. Polypropylene fibres might furthermore be applied satisfactorily for the manufacture of carpets because both in production and in use, less electrostatic charges develop than in other fibres. This, in addition to the fact that walking on the carpet does not generate electric sparks, has the advantage of better soil-resisting properties.

Home experiences in developing the production techniques of polypropylene fibres have considerably facilitated the development of the manufacture of carpet-yarns on polypropylene basis.

A drawback of polypropylene fibres in comparison with polyamides is their slower recovery after deformation. This, however, might suitably be

* A collective study of the Department for Textile Technology and Light Industry at the Technical University, of the Textile Laboratory of the Development and Research Institute of the National Rubber Co. and of the Development and Research Laboratory of the Hungarian Viscose Factory.

influenced — according to our experience — by choosing the right production parameters. The aim of our present investigations was to study the influence of some parameters of the fibre properties on the strength results, to determine the optimum parameters applied in the manufacture. A further target was to choose and develop the adequate methods of testing and evaluation.

2. The experimental spinning and materials tested

2.1 *Spinning*

The fibres investigated were manufactured on the experimental polypropylene spinning equipment of the Hungarian Viscose Factory. The material used was supplied by the Österreichische Stickstoffwerke A.G., in form of Daplen 708/DA polypropylene, with a melting index of 17.2 at 230 °C.

The polymer was melted in a Reifenhäuser extruder type S 60, then the polymer melt was introduced through a heated tube to the spinnerets. The temperatures of the five heating zones of the extruder were:

1st zone	160 °C
2nd ,,	180 °C
3rd ,,	240 °C
4th ,,	280 °C
5th ,,	310 °C

For better homogenizing the polymer melt, the pressure of the extruder was adjusted to 70 att. The temperature of the tube was 250 °C and that of the spinnerets 220 °C.

The temperature of the last zone of the extruder was chosen in order to achieve good flowing conditions and to remove any crystalline knots from the polymer.

Some further characteristics of the spinning:

exit speed of the melt	99 g/min
drawing out speed	270 m/min
temperature of cooling air	21 °C

Fibres produced with the parameters mentioned were let to relax for 48 hours in order to arrive at an equilibrium of the initial crystallisation processes.

2.2 *Drawing and heat setting*

The polypropylene filaments have been processed before drawing on a Dobson & Barlow Crimposet type 983 drawing and texturizing equipment. In this machine filaments undergo a one-scale drawing process. Before entering

the drawing field, filaments are heated up in a first heating field (T_1) to the temperature needed. After leaving the drawing field, filaments enter a second heating field (T_2), where the filament cooled down during the drawing process will be plastified at a temperature ensuring a suitable bulkiness. The repeatedly heated filaments proceed into a crimper with stuffing chamber. After leaving the latter, filaments are straightened on guide-rollers then, to stabilize bulkiness, are heat-set passing several times through heated pairs of rollers (T_f). The extent of drawing for the various specimens and the temperatures applied are shown in Table 1.

Table 1

The extent of drawing the polypropylene filaments and temperatures applied at drawing and heat-setting

No.	Extent of drawing d	Drawing temperature		Temperature of heat setting T_f (°C)	Number of passages on the heated surfaces		
		T_1 (°C)	T_2 (°C)		1	2	3
1	1:3	140	120	120	15	5	3
2	1:3	140	120	135	14	5	8
3	1:3.5	140	120	120	14	5	3
4	1:3.5	140	120	135	14	5	8
5	1:4	140	120	120	14	5	3
6	1:4	140	120	135	14	5	8
7	1:3	140	120	—	14	5	—
8	1:3.5	140	120	—	14	5	—
9	1:4	140	120	—	14	5	—

As shown in the Table, specimens No. 7, 8, 9 were made without heat-setting, specimens No. 1, 3 and 5 were heat-set at a lower temperature and with fewer passages on the heated surfaces, while specimens No. 2, 4 and 6 were set at a higher temperature and with several passages on the heated surfaces. (By this one has tried — as far as possible — to enhance the temperature efficiency at heat-setting.)

2.3 *Some characteristics of the products*

The count of the filament cables produced for the experiments ranged from 460 to 480 tex, the number of capillars was 200.

The melting point of the fibres of all specimens has been 165 °C.

3. Rheological measurements and their interpretation

3.1 *Isothermic rheological measurements*

3.1.1 *Testing apparatus (Rheolometer)*

Rheological measurements were carried out in a Nándory's Rheolometer operated in the textile laboratory of the Development and Research Institute of the National Rubber Co.

The main characteristics of the apparatus are:

clamping length realisable	450 to 600 mm
maximum change of force to be measured	4000 p
treatment temperature	20 to 200 °C
accuracy of measurement	
length	0.05 mm
force	10 p

In deformation tests, tension was applied by means of a hydraulic loading device, in order to prevent sudden shock-like swinging motions.

The apparatus is suitable for change of length measurements at constant loads and for change of load measurements at constant lengths. The programming of the apparatus is effected by hand (control of temperature in function of time, load, etc.).

3.1.2. *Measuring method*

To deal with isothermic tests as to deformation as well as to force tests, temperature was previously adjusted (at ± 2 °C along the length of the clamped yarn). Results on both types of measurements were read off at various intervals, such as 15, 30, 45, 60 sec., 2, 5, 10 and 30 min.

3.1.2.1. *Deformation tests:* in these tests, filaments were clamped with a length of 500 mm and a pre-load of 0.05 p/tex at the testing temperature. During loading, a constant tension of 1 p/tex was applied. The change of length was tested in loaded and unloaded state at the temperatures of 20, 60, 80 and 100 °C.

3.1.2.2. *Force tests:* tests were carried out with a constant clamped length of 500 mm, under a pre-tension of 0.05 p/tex. Testing temperatures: 60, 80, 100 and 120 °C.

3.2 *Deformation tests*

3.2.1. *Test results*

Figs 1 to 9 show the yield and recovery of deformation curves for the 9 sorts of polypropylene filaments, in space co-ordinate system. On the three co-ordinates were plotted: the deformation (ε%), the temperature (T °C) in

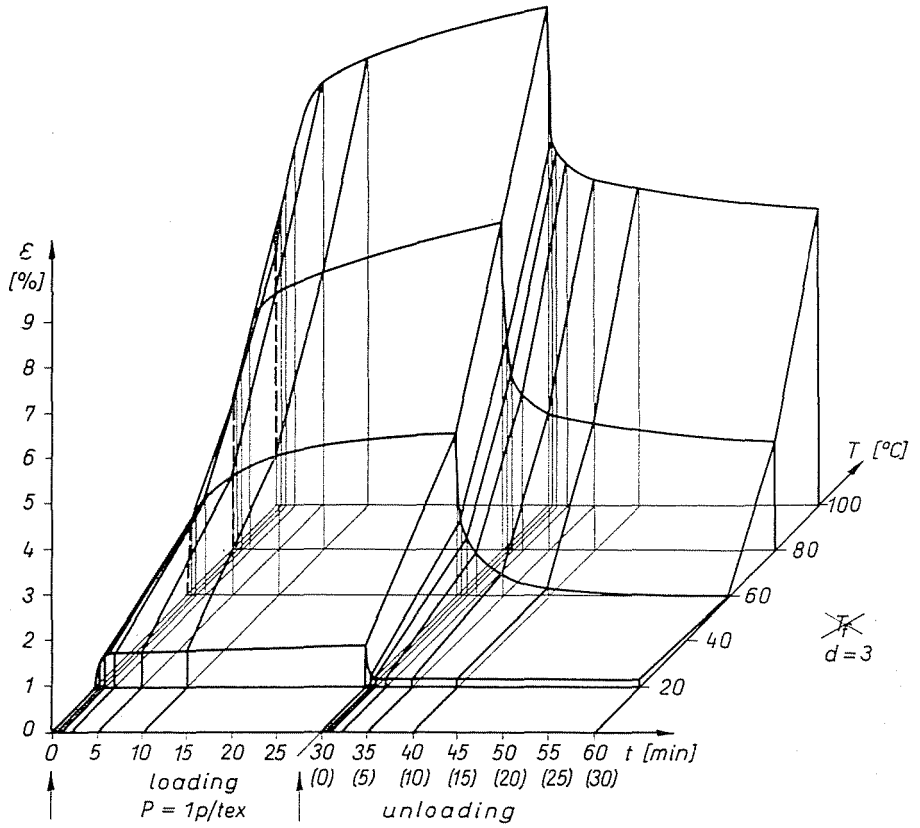

Fig. 1. Yielding and deformation recovery curves of specimens made with draft $d = 3$, without heat setting, at various testing temperatures

function of time (t min.). On the t axis can therefore be read the isothermic changes, while on the T axis the isochronic ones. (The figures show also the shrinking zones.)

As seen by the diagrams, the line of the yield (loading) zone is conventional, no detailed comments are needed. The recovery curves, however, are much more interesting in the unloading zone, they being a textile technological concept of decisive importance from the aspects of both processing and performance.

This is why we shall only deal further on with the recovery from deformation.

For an additional analysis, this conventional way of graphic presentation was completed by means of analyses described further on.

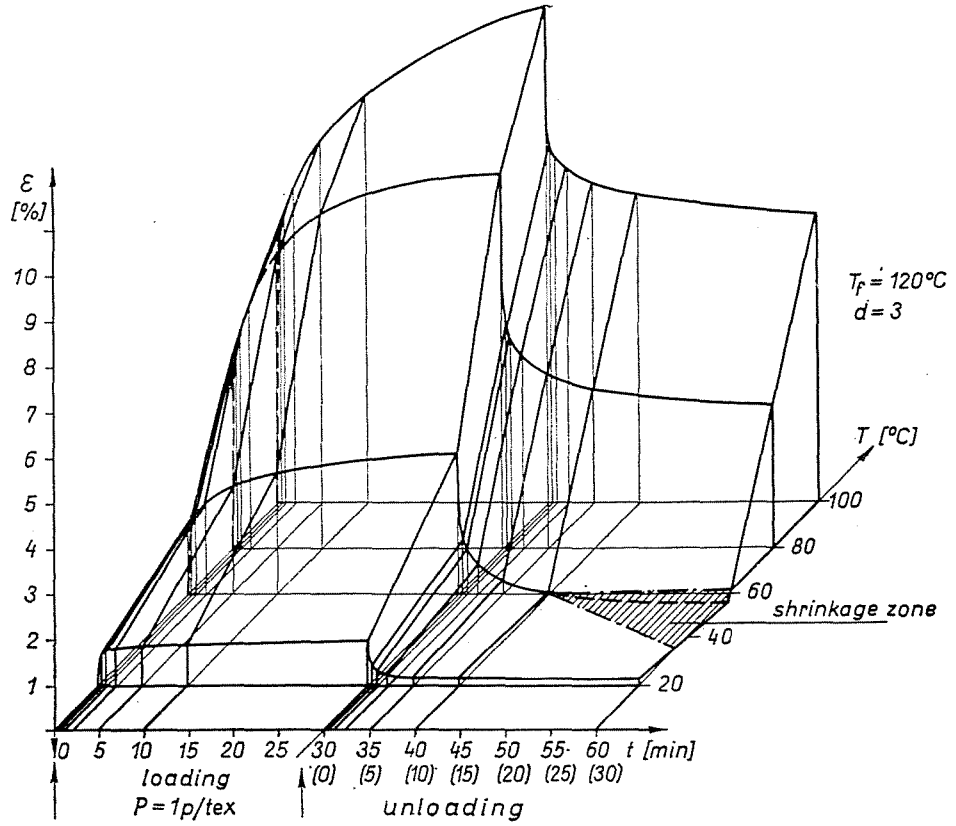

Fig. 2. Yielding and deformation recovery curves of specimens made with draft $d = 3$ and heat-set at $T_f = 120$ °C, at various testing temperatures

3.2.2. *Correlation between relative recovery and time factor*

If one replaces the above mentioned absolute deformation value (ε) by another one representing relative recovery, giving essentially useful information on the behaviour of the filaments tested in the unloading zone, the correlation between relative recovery and time might be characterized as follows:

First of all, in order to ensure unequivocal discussion the following symbols will be introduced:

$$\lambda_{ik} = \frac{l_{0k} - l_{ik}}{l_{0k}} = \frac{\varepsilon_{0k} - \varepsilon_{ik}}{1 + \varepsilon_{0k}}$$

where λ_{ik} — the relative recovery at time $t = i$ and temperature $T = k$
l_{0k} — the length of the cable at the moment of unloading ($t = 0$) at temperature $T = k$

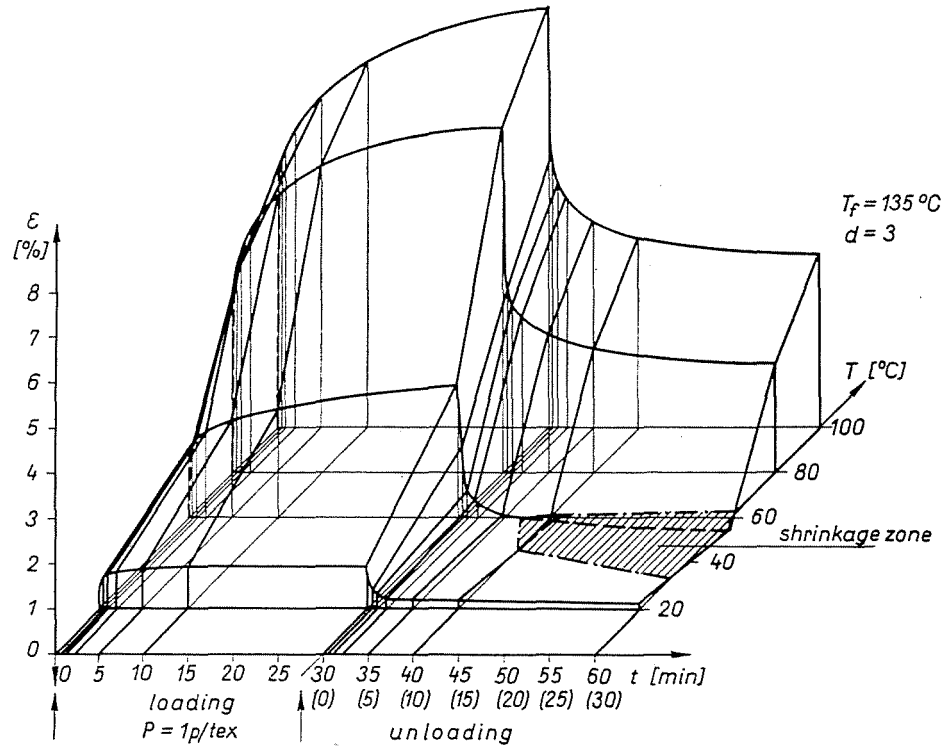

Fig. 3. Yielding and deformation recovery curves of specimens made with draft $d = 3$ and heat-set at $T_f = 135$ °C, at various testing temperatures

l_{ik} — the same at time $t = i$
ε_{0k} — deformation at time $t = 0$ at a temperature $T = k$
ε_{ik} — the same at time $t = i$

Fig. 10 shows the empirical relationship

$$\lambda_{ik} = f\ (\lg\ t)$$

for all the nine specimens.

According to the diagram, the highest relative recovery is observed generally at 60 °C. This fact will still more strikingly be seen from the picture to be described later on.

The relation between relative recovery and the logarithm of time can in many cases be regarded as linear. This is valid especially for the behaviour of materials made with a draft of $d = 3$ and $d = 4$ and of filaments with a draft of $d = 3.5$ at room temperature and, in some cases, at 100 °C.

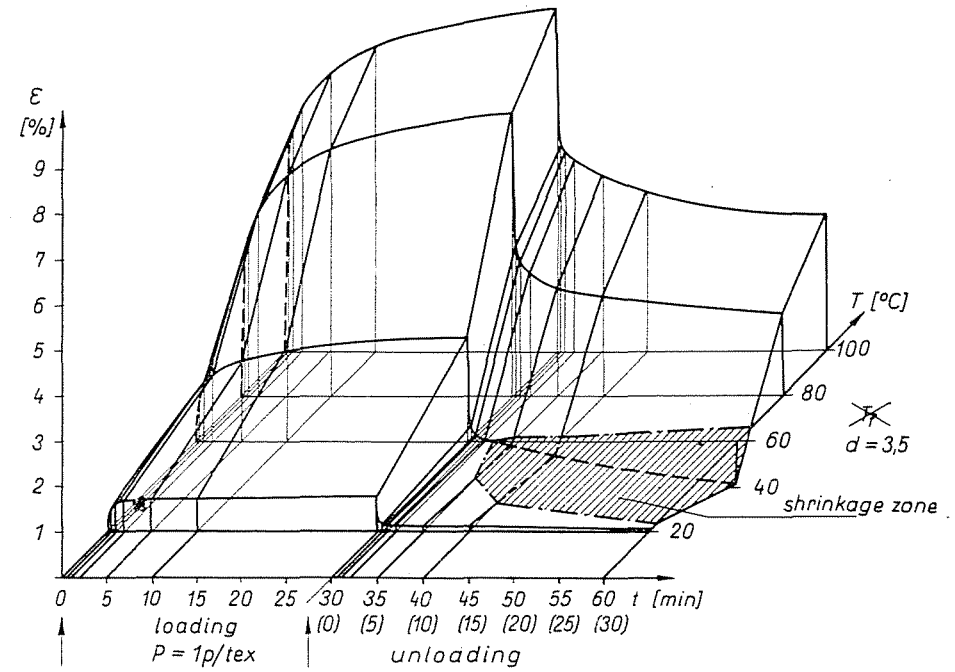

Fig. 4. Yielding and deformation recovery curves of specimens made with draft $d = 3.5$ without heat-setting, at various testing temperatures

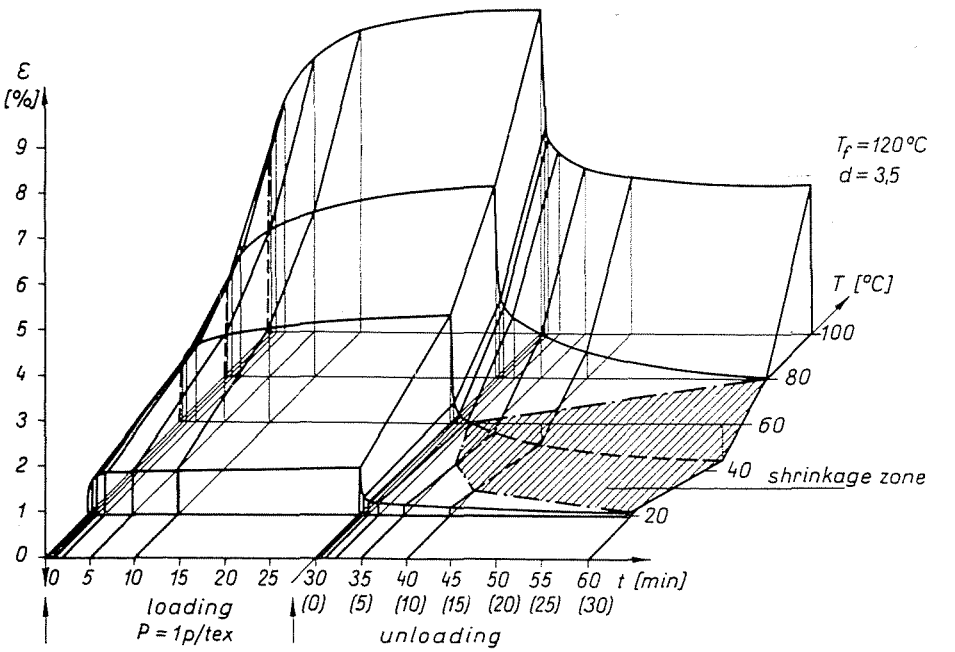

Fig. 5. Yielding and deformation recovery curves of specimens made with draft $d = 3.5$ and heat-set at $T_f = 120$ °C, at various testing temperatures

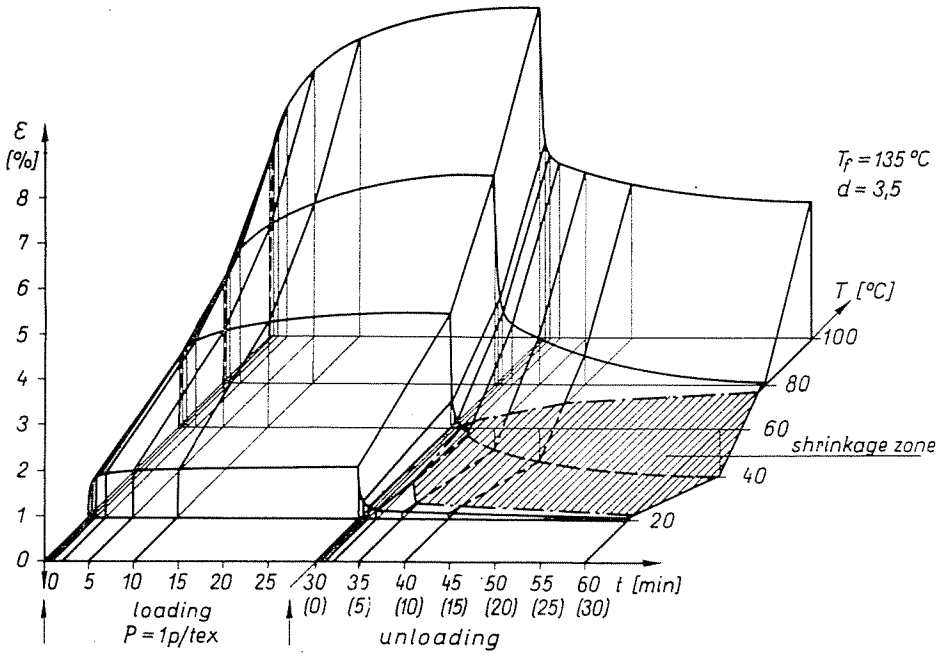

Fig. 6. Yielding and deformation recovery curves of specimens made with draft $d = 3.5$ and heat-set at $T_f = 135$ °C, at various testing temperatures

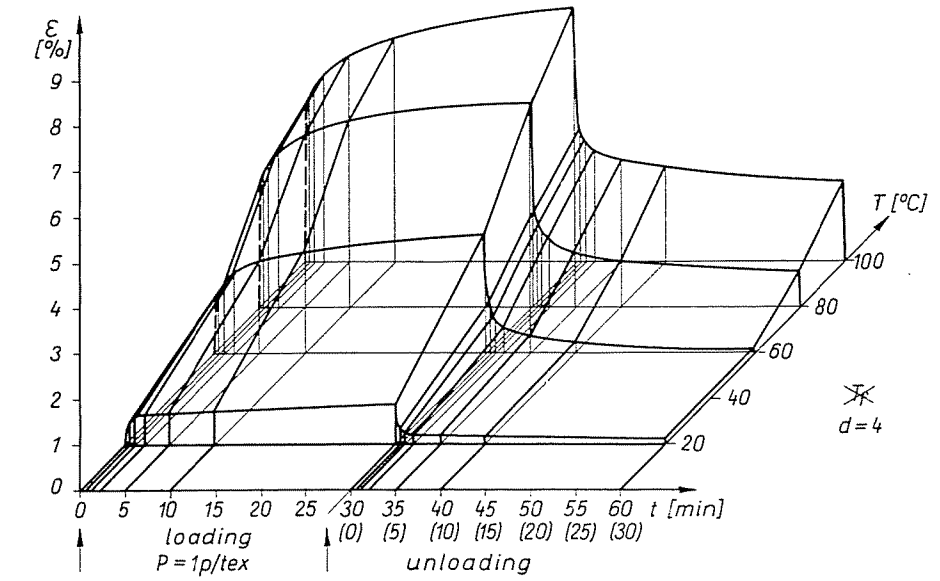

Fig. 7. Yielding and deformation recovery curves of specimens made with draft $d = 4$ without heat setting, at various testing temperatures

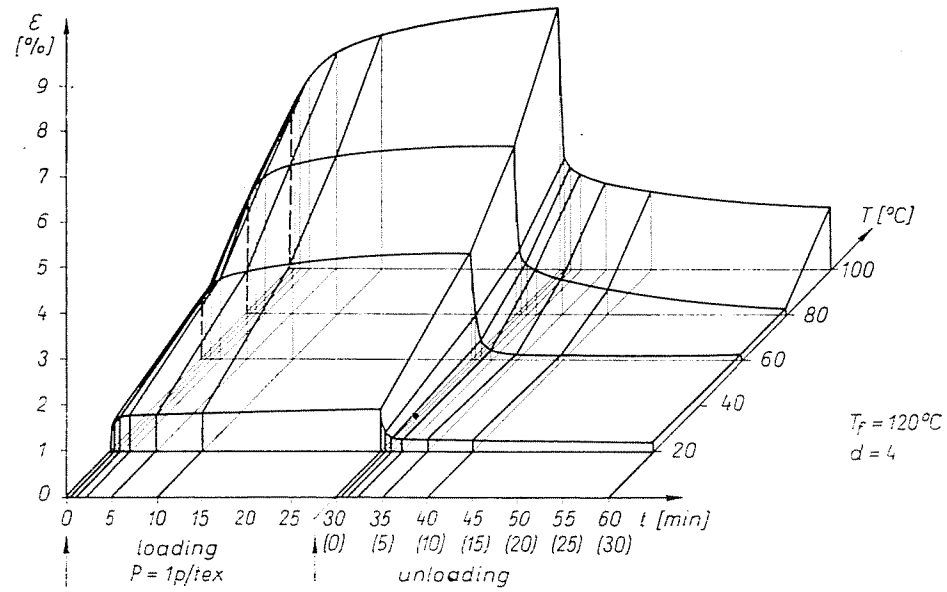

Fig. 8. Yielding and deformation recovery curves of specimens made with draft $d = 4$ and heat-set at $T_f = 120$ °C, at various testing temperatures

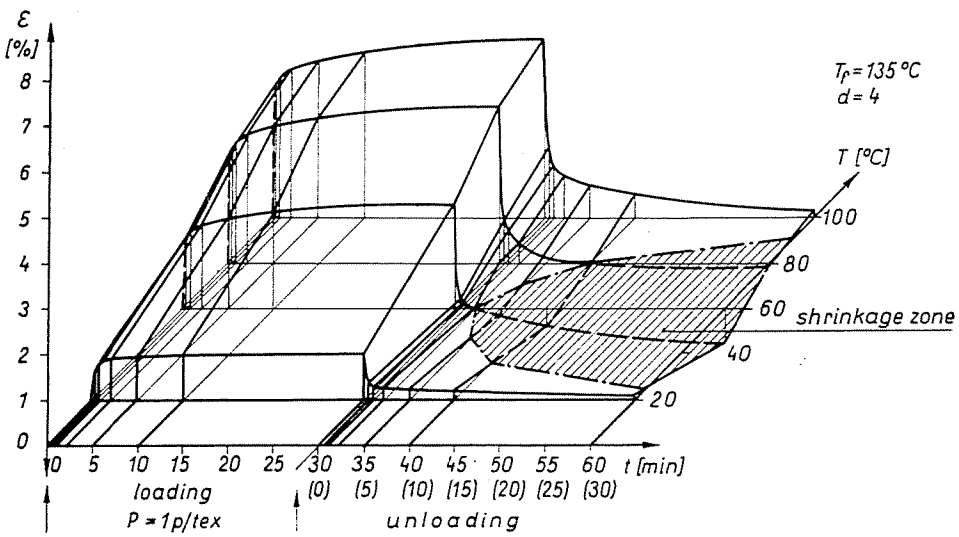

Fig. 9. Yielding and deformation recovery curves of specimens made with draft $d = 4$ and heat-set at $T_f = 135$ °C, at various testing temperatures

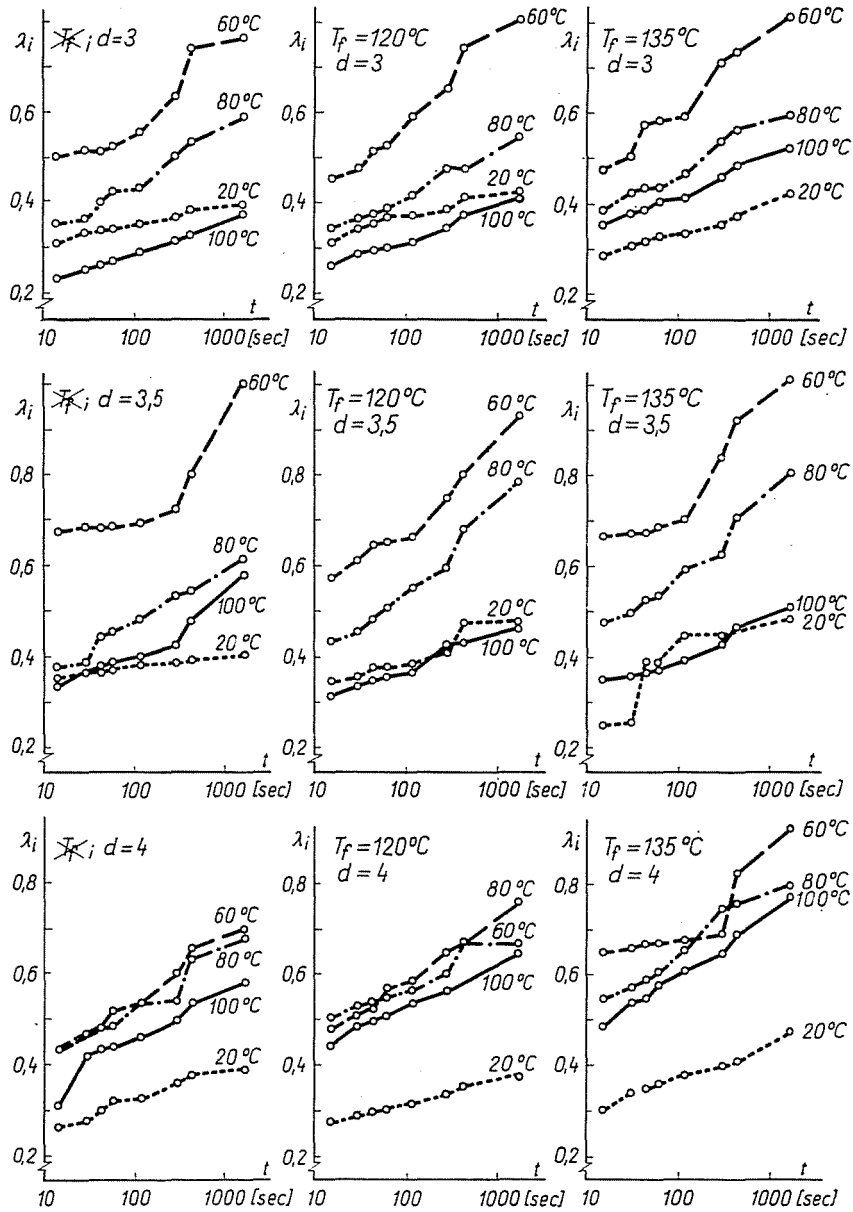

Fig. 10. The $\lambda_i = f(\lg t)$ relation, viz. the change in relative recovery in function of the logarithm of relaxation time

3.2.3. *Correlation between relative recovery and temperature*

Fig. 11 shows diagrams representing the change of relative recovery in function of time at certain characteristic instants. On the diagrams changes of length at 15 sec, 1, 5, and 30 min were plotted. The following conclusions can be drawn therefrom:

— in most of the cases a decisive maximum can be seen at about 60 °C with all specimens tested, as has been mentioned before (exception: specimen with $d = 4$ drawn at $T_f = 120$ °C),
— in most of the cases, the form of the curves shows a similar tendency for the various materials, which means that recovery properties of the different specimens will not considerably be modified in function of time.

3.2.4. *The effect of drawing and heat-setting temperature on recovery performance*

Fig. 12 contains data plotted vs. time related to relative recovery at $t = 30$ min (λ_{ik}) to deformation after 30 min (ε_{ik}) and to deformation at the instant of unloading (ε_{0k}). For each series of diagrams the heat-setting temperature was regarded as constant.

In Fig. 13 similar parameters are shown at various drafts. Thus, in Fig. 12 each vertical series of diagrams represents parameters of specimens without heat-setting, and heat-set at 120 °C and 135 °C temperature, respectively, with various drafts. On Fig. 13, however, each vertical group of diagrams shows the characteristics of specimens with drafts of 3, 3.5 and 4, at different heat-setting temperatures, and without heat-setting, respectively.

Conclusions:

— relative recovery will not considerably be influenced by heat-setting temperature or by dropping heat-setting;
— the values for ε_{ik} as well as for ε_{0k} show a certain decreasing tendency at higher heat-setting temperatures;
— the maximum shrinkage and minimum deformation will generally be found, as already stated, at about 60 °C.

The highest relative recovery up to about 80 °C will be at a draft of $d = 3.5$, while at 100 °C the maximum will always appear at a draft $d = 4$. Accordingly, the minimum of permanent deformation in 30 min. will, up to 80 °C, be observed at $d = 3.5$ or $d = 4$, beyond this temperature in every case at $d = 4$.

In comparison to the influence of the change of draft, the effect of heat-setting temperature is negligible. This becomes clear from comparing the two pictures.

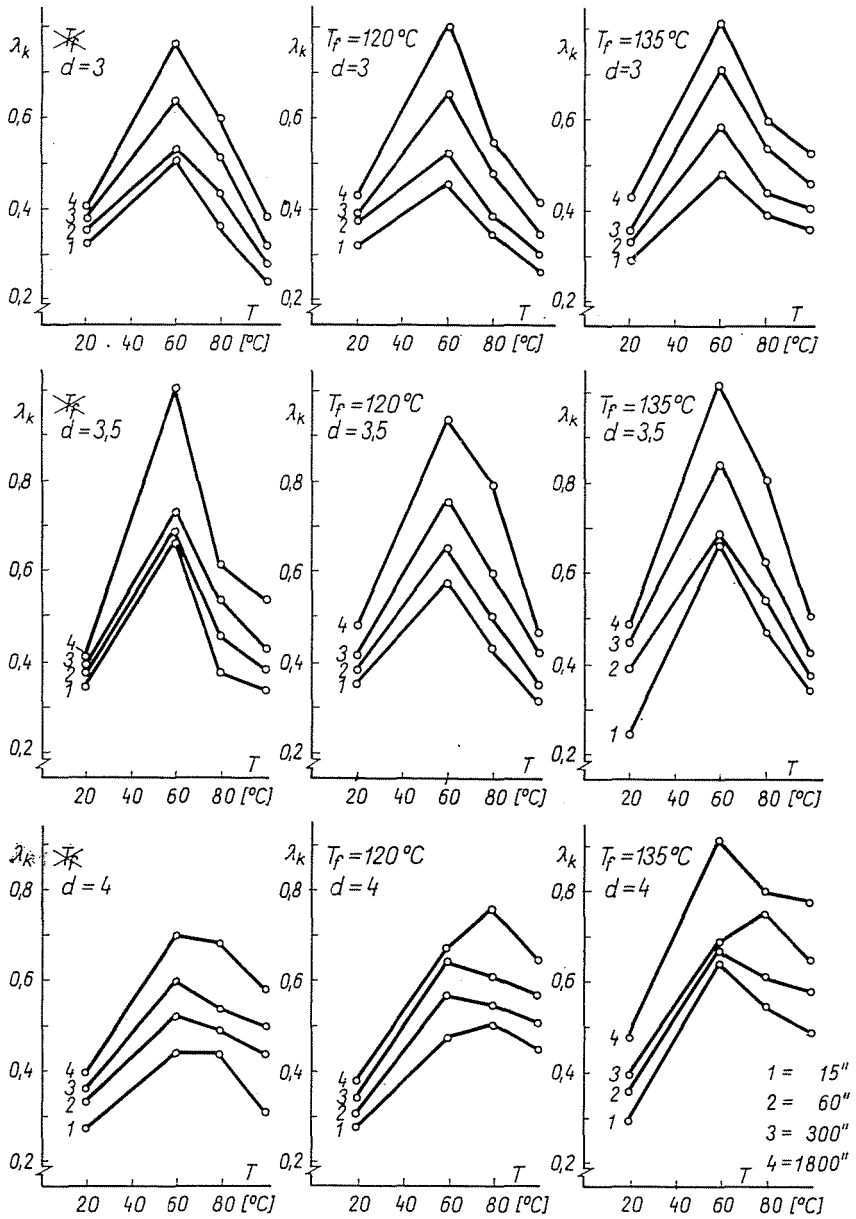

Fig. 11. The $\lambda_k = f(T)$ relation, viz. the change in relative recovery in function of the temperature

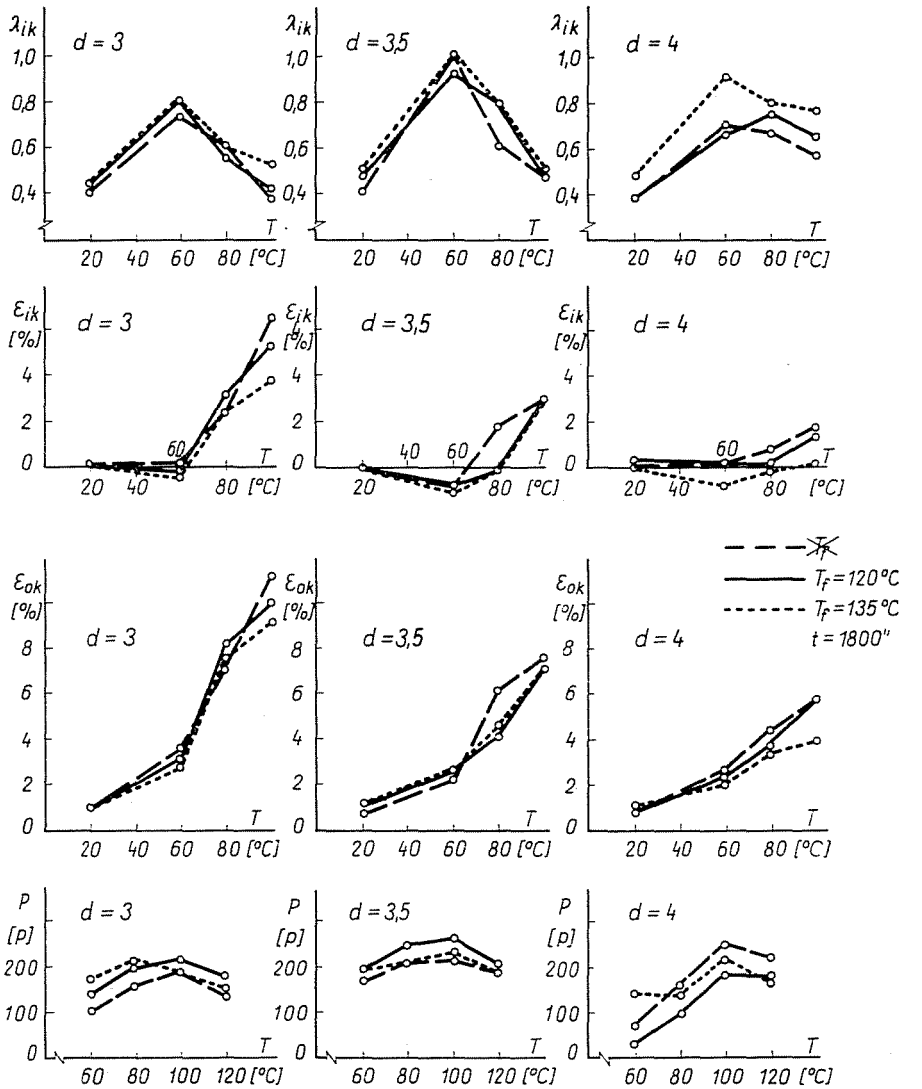

Fig. 12. The change of relative recovery in $t = 30$ min (λ_{ik}), of deformation occurring after 30 min (ε_{ik}), of the deformation observed at the moment of de-loading (ε_{0k}) and of the shrinking force (P) in function of the temperature. (At various heat-setting temperatures)

On the strength of the two concepts (viz. influence of the heat-setting temperature and of the draft) recovery performances of the tested nine filaments were evaluated under the test conditions. For the sake of analysis the following factors have been determined [3]:

time factor of recovery

$$A_t = \frac{\varepsilon_{ik}}{1+0.01\,\varepsilon_{0k}}$$

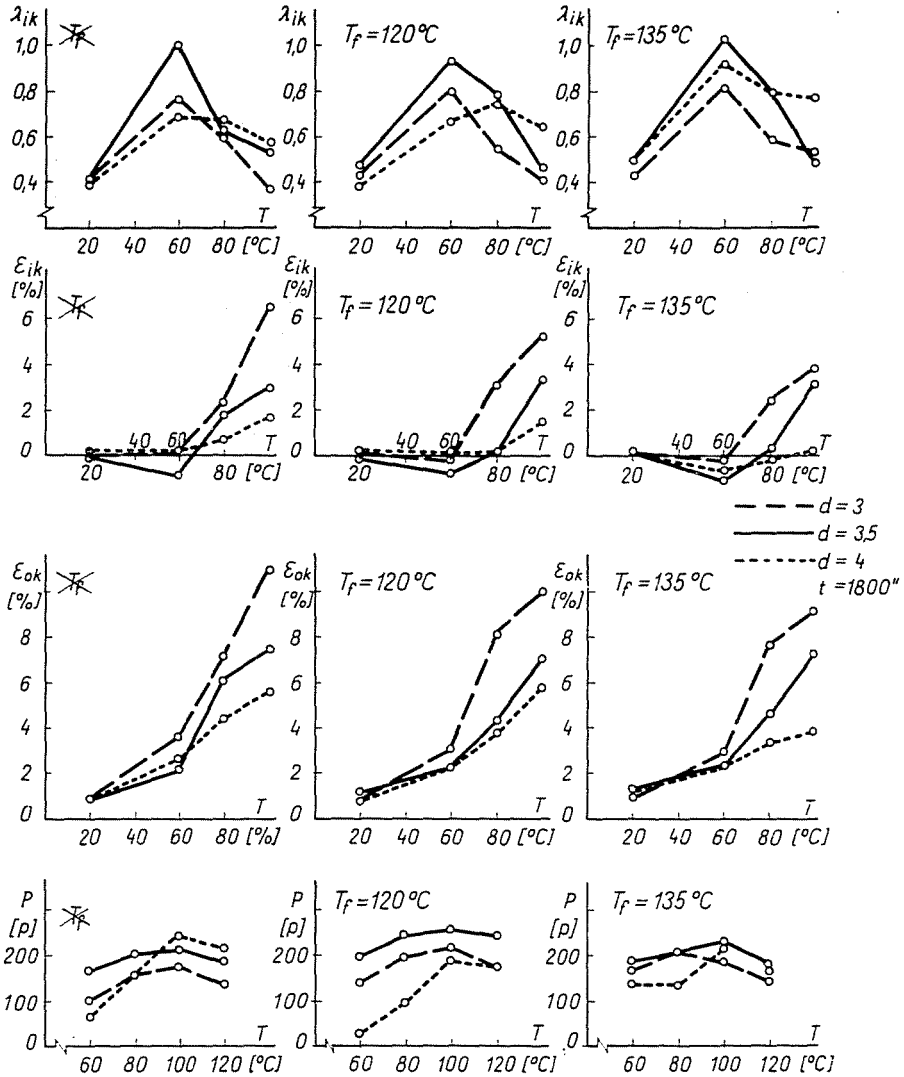

Fig. 13. The change of the factors λ_{ik}, ε_{ik}, ε_{0k} and P in function of temperature at various drafts

factor of heat stability

$$\Lambda_t = \varepsilon_{i0} - \varepsilon_{ik}$$

recovery index

$$\Lambda = |\Lambda_t| + |\Lambda_T|$$

where:

ε_{i0} — deformation at the basic temperature (in our case 20 °C) at instant $t = i$

In connection with the three factors mentioned above, the following remarks should be made:

— from the viewpoint of recovery performance that product will be the better for which, at a given instant and temperature, the dimension under load will be nearer to its initial dimensions, considering also deformation at unloading;

— from the viewpoint of heat stability, that product will be better, which, at a given instant, will be less sensitive to temperature changes.

Both factors represent a certain deformation which is characteristic of the product as dependent from time on the one hand and from temperature on the other. Attributing equal importance to both factors, *then, and only then*, can recovery index be applied.

On the strength of the formulas given we should remark the following:

— as to the time factor of recovery:
as $\varepsilon_{0k} > 0$, and $\Lambda_t \gtreqless 0$ depending on $\varepsilon_{ik} \gtreqless 0$, if $\varepsilon_{ik} \to 0$, $\Lambda_t \to 0$

— as to the factor of heat stability:
if $\varepsilon_{ik} \to \varepsilon_{0k}$, then $\Lambda_T \to 0$

— as to the recovery index: if $\Lambda_t \to 0$ and $\Lambda_T \to 0$, then $\Lambda \to 0$

All this shows that when evaluating the various specimens, from the aspect of recovery performance that sample will be the better which in its absolute value will be nearer to 0.

In Fig. 14 the values of the three factors have been plotted according to heat-setting temperatures so that each vertical group of diagrams contains the three factors as a function of temperature at various drafts.

In Fig. 15 the changes of the three factors have been represented similarly at constant drafts according to the various heat-setting temperatures.

From both diagrams our above mentioned statements can in their synthesis be proved.

There is a rather close relationship between the recovery time factor and the factor of heat-stability. This also points to the fact that recovery performance of various products will in the first instance be determined by the change of testing temperature. The picture shows furthermore that deformation recovery of polypropylene filaments will in every case be rather good at low temperature.

As regards recovery time factor, the best specimens at lower temperatures (up to 60 °C) are the products drawn at $d = 3$ and $d = 4$, at temperatures between 60 °C and 100 °C are those made with a draft of $d = 4$. In connection of heat stability factor, similar conclusions may be drawn. This statement is in accordance with that arrived at previously as regards highest relative recovery at a draft of $d = 3.5$.

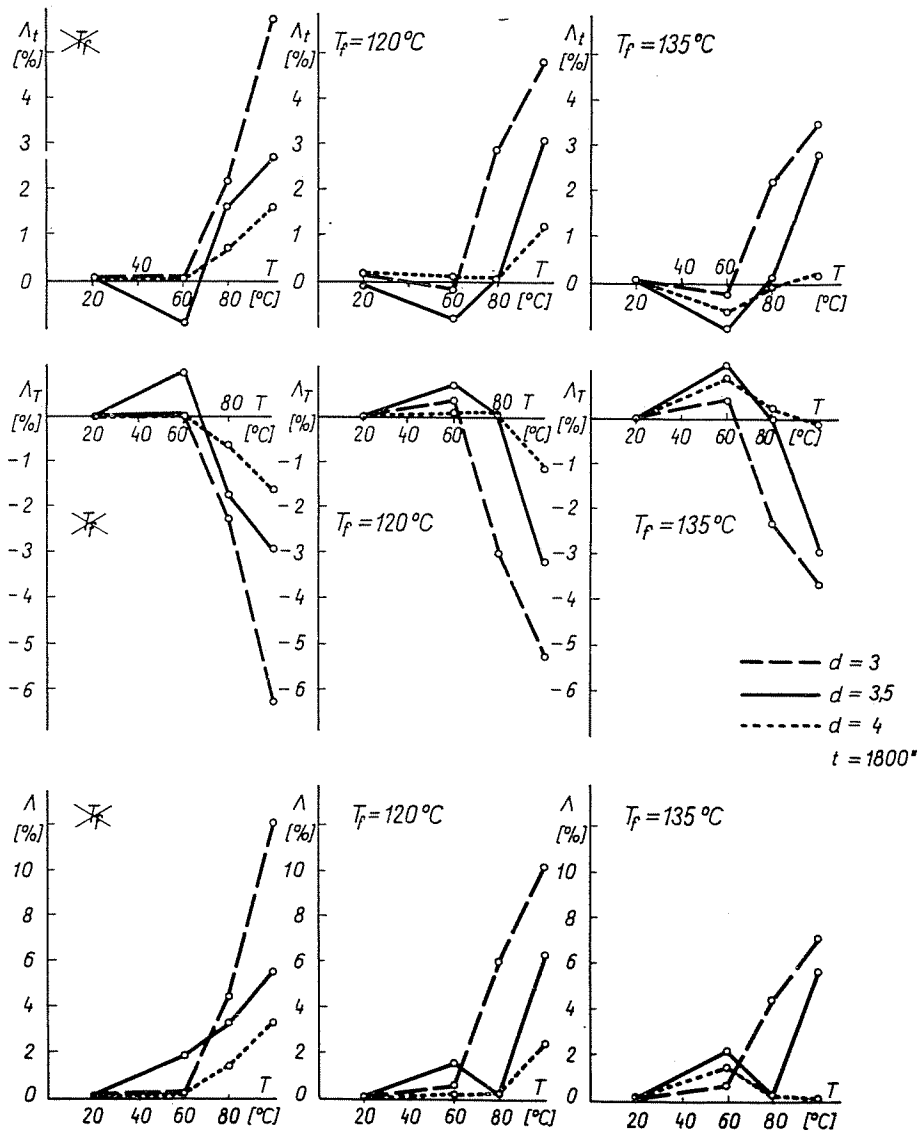

Fig. 14. The time factor of recovery (Λ_t), the factor of heat-stability (Λ_T) and recovery index (Λ) at constant heat-setting temperature and at various drafts

It should be pointed out that — as it was to be expected — with specimens without heat-setting the greatest absolute value of shrinkage was to be observed at the variety made with a maximum draft. In case the product will be heat-set, the previous statement will be valid as regards draft of $d = 3.5$.

It should also be emphasized that at a temperature over 80 °C the

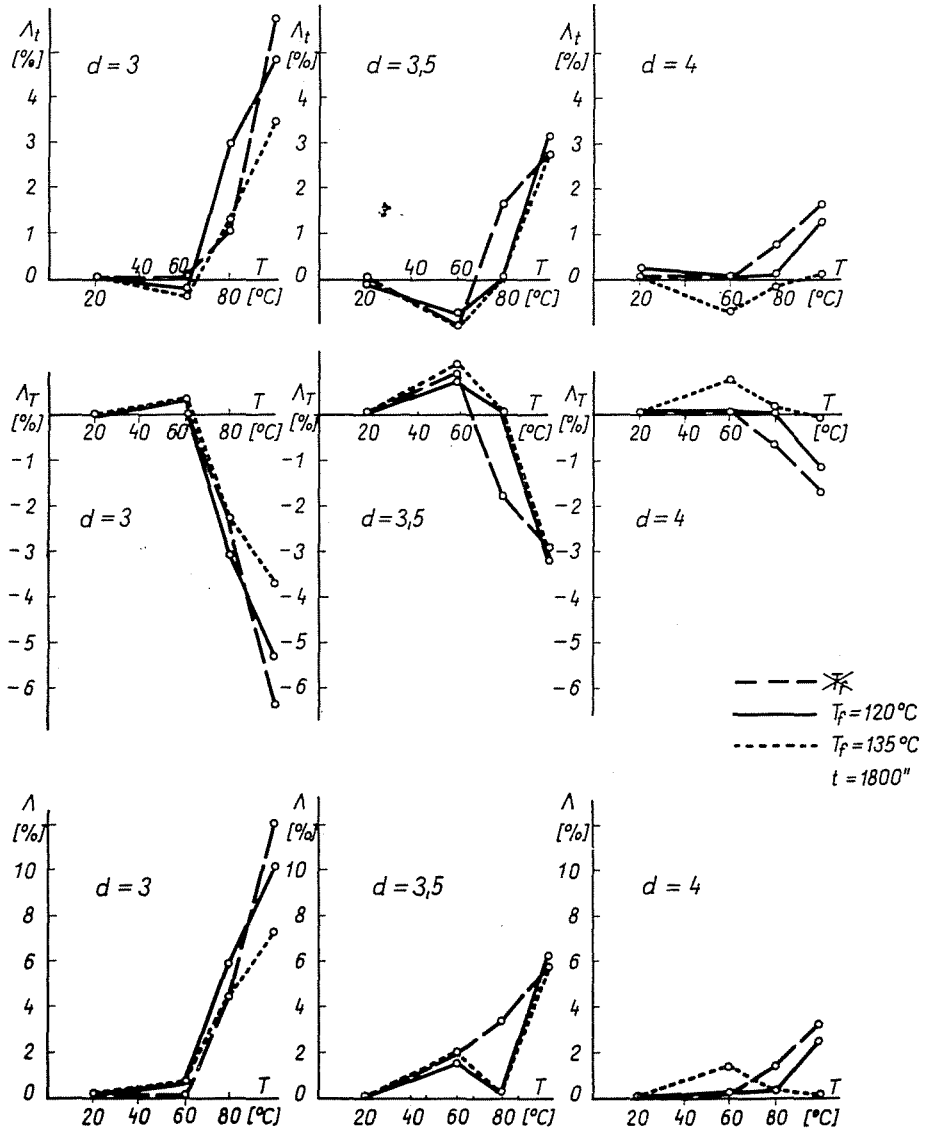

Fig. 15. The change of the factors Λ_t, Λ_T and Λ at constant drafts and various heat-setting temperatures

material gets quickly deformed, while at higher draft somewhat less quickly. Raising the heat-setting temperature improves to a certain extent the recovery performance *in case it is concomitant to a higher draft.*

It should finally be noted that at 100 °C the absolutely best result in all the three factors was obtained with products heat-set at a temperature of 135 °C and drawn at $d = 4$.

3.3. *Force tests*

By the method described in section 1, the shrinking force has been determined in the mentioned temperature range of 60 to 120 °C. As shown in Figs 12—13 the shrinking force shows (in most of the cases) a maximum at 100 °C. It is to be surmised that over this temperature such structural changes take place in the material, which, in the end, lead to the complete disappearance of the shrinking force and to the rupture (melting) of the cable.

The maximum value of the shrinking force — which can be put to about 0.5 p/tex — does not show any considerable change in function of the various products made with different parameters. There is, however, a very close correlation to be observed between the relative recovery and the shrinking force as — at the different heat-setting temperatures — the maximum shrinking force and the maximum of the relative recovery will be found at a draft of $d = 3.5$.

It can be stated at the same time that while for the recovery from deformation the extent of draft was the decisive factor, the value of the shrinking force will equally be influenced both by the extent of draft and by the heat-setting temperature.

4. Modelling of the rheological processes and determination of the material constants

For the demonstration and thorough analysis of the stress-strain mechanism in visco-elastic materials a considerable help is given by the rheological analogous models constructed by some of the researchers (KELVIN, MAXWELL, VOIGT, KUKIN-SOLOVEV). The mathematical models attached to the rheological ones generally enable to establish numerical values of the material constants characterizing this mechanism.

A better-known group of analogous models are the mechanical ones; these are built up by a combination of springs and values containing viscous liquids. Among the various members of the model springs are characterized by their elastic modulus (E) while the valves by the viscosity factor (η) of the liquids they contain.

In the special literature, mention is made of electrical analogous models [8, 9]. In these the springs of the mechanical analogous models are replaced by condensers, the valves containing viscous liquids by resistances, for analoguing the stress and deformation, the current intensity and the electric tension, respectively, are being used. According to this, e.g. the so-called momentaneous elastic elongation, symbolized in mechanical models by instantaneously elongating springs, will be analogued by a condenser; it is supposed that it takes up its charge at a time $t = 0$, which is physically

impossible (and excludes at the same time the actual technical realisation of the model).

The rather contrarious requirements toward analogous models are: they should model the performance of polymers with a good approximation and, at the same time, they should not be too complicated, too complex. If a numerical interpretation of the test results is needed, then simplicity of the model is of outstanding importance. Namely it is well known that to even relatively simple models complicated (mostly transcendent) equations belong, of which even the approximate solution is rather tiresome.

The well-known mechanical and electrical analogous models will only be used for calculations and to establish relationships between some material and rheological characteristics. The literature does not report on model constructions actually realised.

To facilitate analytical and demonstrative work as to rheological tests of textiles, an electrical analogous model has been constructed at the Budapest Technical University [10, 11] which could technically be realised and was suitable for the following purposes:

— to model the stress-strain mechanism of visco-elastic material under quasi-static conditions;

— for the comparative analysis of the phenomena described by various analogous models and of actual test results, moreover to try out new modelling possibilities beyond those already known;

— for the analysis and for a quick numerical interpretation of the equations related to the models and to the relaxation and retardation performance of textiles; respectively after selecting (or establishing) a suitable model construction.

We did not intend in the first instance to increase the number of rheological models by our research work, but wanted rather to establish an electrical analogous model enabling us to select a kind of construction best approximating the actual test results.

4.1. *Description of the electrical analogous model*

We have chosen the following electrical analogies as the basis of our model:

Mechanical terms		*electrical analogy*	
σ	(tension)	$= I$	(current intensity)
ε	(elongation)	$= U$	(tension)
E	(elasticity modulus)	$= \frac{1}{R}$	$\frac{1}{\text{(resistance)}}$
η	(viscosity)	$= C$	(capacity)
t	(time)	$= t'$	(time)

A great advantage of the electrical analogies selected is that the electrical parameters of our construction describe certain relations of stress-strain and material constants in a similar way as the parameters of mechanical models do, which means that their mathematical models are identical (Figs 16, 17 and 18). Moreover, the fact that in our model, as differing from the electrical

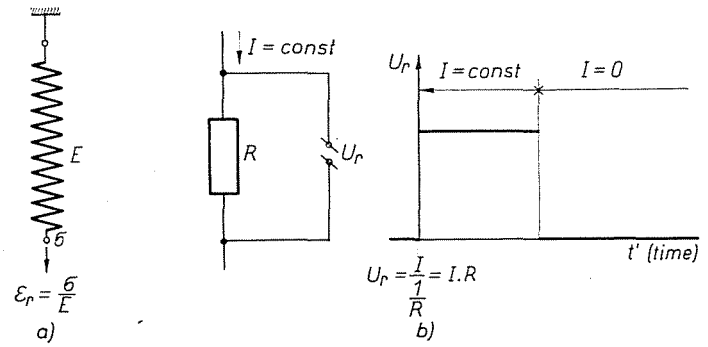

Fig. 16. The mechanical (a) and electrical (b) analogizing of the momentaneous elastic elongation (ε_r)

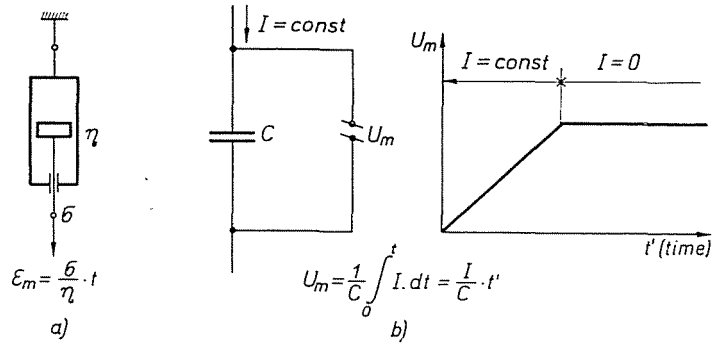

Fig. 17. The mechanical (a) and electrical (b) analogizing of the permanent elongation (ε_m)

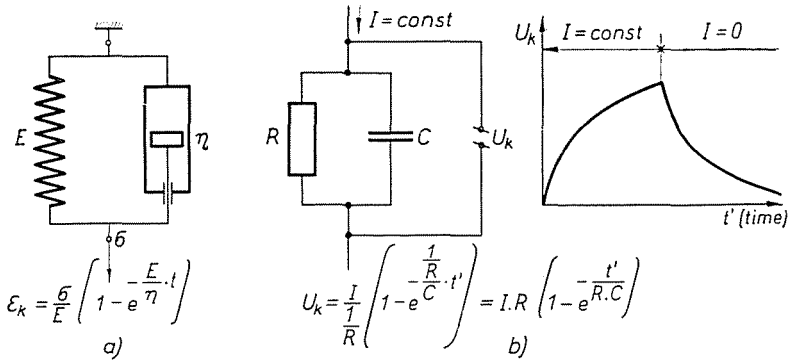

Fig. 18. The mechanical (a) and electrical (b) analogizing of the retardated elastic elongation (ε_k)

analogy dealt with in trade-literature, the springs of mechanical models are represented by resistances, the valves by condensers, the technical possibility of their realisation is ensured, maintaining at the same time the correctness of the analogy.

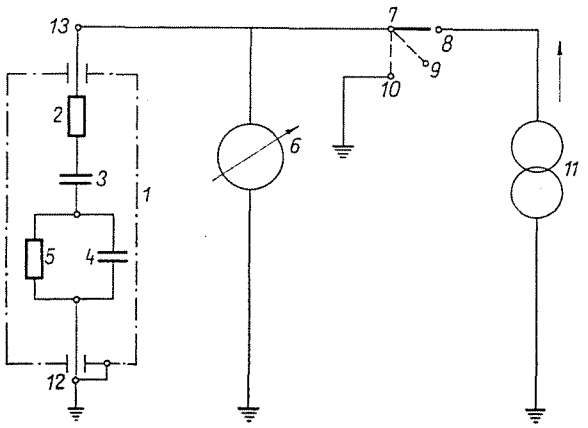

Fig. 19. Connection skitch showing the operation in principle of the electrical model-construction

According to the chosen electrical analogies, e.g. the characteristic equation of the "yield" phenomenon described by the so-called four-parameter mechanical model composed by elements of Maxwell and Kelvin under conditions ($\sigma = \text{const.}$, $\varepsilon = f(t)$):

$$\varepsilon = \frac{\sigma}{E_1} + \frac{\sigma}{\eta_1} \cdot t + \frac{\sigma}{E_2}\left[1 - e^{-\frac{E_2}{\eta_2} \cdot t}\right] \tag{1}$$

will be modified as follows:

$$\begin{aligned} U &= \frac{I}{1/R_1} + \frac{I}{C_1} \cdot t' + \frac{I}{1/R_2}\left[1 - e^{-\frac{1/R_2}{C_2} \cdot t'}\right] = \\ &= I \cdot R_1 + \frac{I}{C_1} \cdot t' + I \cdot R_2\left[1 - e^{-\frac{t'}{C_2 R_2}}\right]. \end{aligned} \tag{2}$$

The principles of operation of our model-construction are shown by the schematic diagram in Fig. 19 (representing the electrical analogy of the so-called four-parameter mechanical model).

In this figure, the model with the required characteristics is represented by resistances 2 and 5 put into the shielding cup 1 and by condensers 3 and 4. The model which can arbitrarily be established is inserted between points 12 and 13. The temporal change of the potential of point 13 will be registered by the voltmeter 6. The "static" operation of the model for the reproduction of yield and recovery curves will be as follows:

a) If switch 7 is turned into position 8, direct current 11 will start the charging process of the model. (In a mechanical sense this corresponds to the so-called loading section as described by Eqs (1) and (2).) The temporal change of the tension will be registered in this and in the following cycles by voltmeter 6.

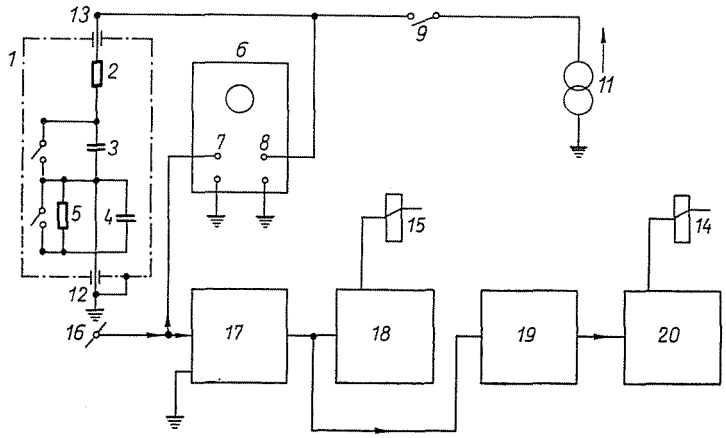

Fig. 20. Blocking sketch of the electrical model-construction

b) If switch 7 is turned into position 9, the process of charging will be interrupted. (In a mechanical sense this corresponds to the so-called unloading section.)

c) If switch 7 turned into position 10, the discharge begins (the discharge of the condensers of the model) to establish initial stage. (This cycle has naturally no mechanical analogy.)

The connection diagram in Fig. 19 is only to show the principles of operation. The electrical representation of the processes "loading and unloading" by means of this method — called "static" by us — is practically difficult. By the periodic repetition of the phenomenon, however, an easy registration may be ensured and, in addition, in this case there arises a possibility to apply easily realisable model elements.

Fig. 20 contains a block-sketch of our electrical analogous model. The device is built up by decades of resistance 2 and 5, of condenser decades 3 and 4 into a so-called four-parameter model* and will undergo periodically and repeatedly the following actions:

— charge (from direct current 11)
— intermission of the charging process
— discharge of the condensers.

* The model described should be regarded as an example.

The potential of point 13 of the model will be registered by 6 cathode-ray direct-current oscilloscopes. (The quick repetitions ensure a "still".) An electronic control device ensures the periodical operation. (Control is carried out by a multivibrator synchronised with the sweep circuit of the oscilloscope.)

4.2. *The process of plotting a four-parameter analogous curve*

Thus, by means of the model-construction, the yield and deformation recovery curves of textiles can — under almost arbitrary conditions and types of model — be reproduced (and simulated). This ensures also an easy and quick method for the analysis of these curves; from the yield and deformation recovery curves plotted by usual measuring methods, our device will in a short time determine the material constants connected with the rheological model applied, besides to permit a rapid approximate solution of equations — generally transcendent ones. For this purpose it is only necessary to plot to a right scale an "analogous curve" covering the measuring curve — after assembling the required model from the condenser and resistance decades — and to read the corresponding parameters, material constants, on the setting organs of the device.

Fig. 21 shows the practical way to trace the analogous curve — and at the same time to determine the material constant — when applying a four-parameter model.

The steps of the procedure are:

— the curve $\sigma = \text{const.}$, $\varepsilon = f(t)$ will be traced arbitrarily (Fig. 21a) on a tracing paper to a scale which permits to show on the screen of the oscilloscope and then the drawing should be put on the screen of the oscilloscope taking good care that the corresponding axes should cover each other;

— the series connected resistance decade — symbolizing the momentaneous elastic elongation — will be switched on and the required drop of voltage will be set by changing the resistance (Fig. 21b), thus one obtains the numerical value characteristic of the momentaneous elastic elongation;

— the series connected condenser decade — symbolizing the permanent elongation — will be switched on and the value of the capacity so adjusted that the line of condenser charge vs. time is parallel to the tangent of the curve at its end point (Fig. 21c), thus one obtains the numerical value characteristic of the permanent elongation;

— the resistance and condenser decades connected in parallel symbolizing the retarded elastic elongation will be switched on and the value of the capacity and resistance necessary of covering the curve (Fig. 21c), thus the numerical value of the two parameters characteristic for the retarded elongation will be obtained. (In course of forming the analogous curve, essentially the parameters of Eqs (1) and (2) have been determined.)

In accordance to the above-mentioned principles the yield section (loading cycle) of the empirical curve (Fig. 21a) has been analysed. The deformation recovery section (unloading cycle) should be electrically formed and analysed, respectively, in a separate operation but adhering to the above principle. The material constants determined by means of these two sections

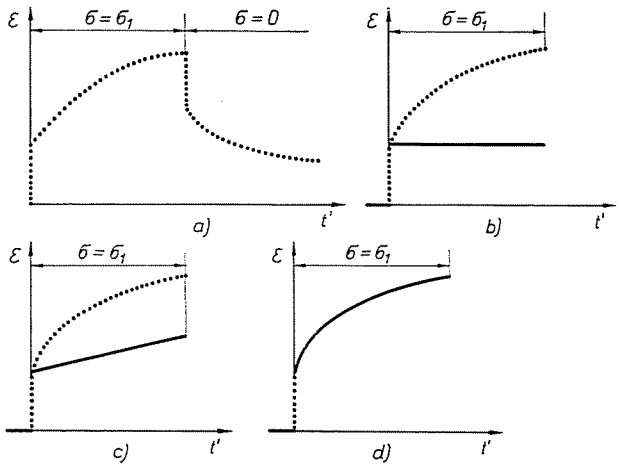

Fig. 21. The sections of forming the electrical analogous curve

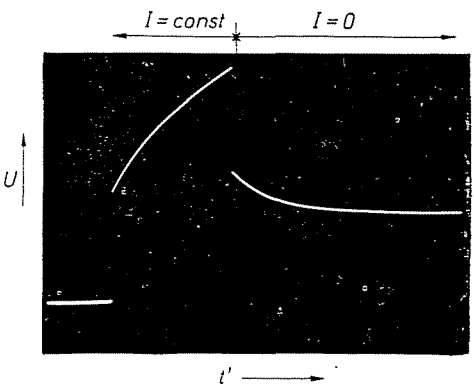

Fig. 22. Electrical analogous curve

of the curve are different. (These differences between the material constants — as is generally known — give an information on the previous history of the visco-elastic material tested.)

Fig. 22 shows the picture of the oscilloscope screen of our device. (By means of a four-parameter model the yield and deformation curves of polyethylene wire were demonstrated on the screen. The picture shows the appearance and good visibility of the curves.)

4.3. *Results of the analyses carried out by the model construction*

By means of our model construction — at four-parameter analogy — retardation curves of our specimens traced under isothermic conditions, at various testing temperatures were analysed (Figs 1 to 9), viz. the material constants characterizing the retardation behaviour were determined. The yield section in course of loading and the recovery from deformation during unloading have been analysed separately; the material constants determining the two sections, depending upon the pre-treatment, especially that of heat-treatment, being different. (According to our findings, the viscosity factors have, in the first instance, shown a marked difference, thus they pointed more to a "heat-history".)

The results of our analyses have been collected in Tables 2, 3, and 4. The values of the material constants belonging to the yield and deformation recovery curves traced at a test temperature of 22 °C were also shown in a diagram; it was at this temperature that the material constants have shown the most considerable change. Figs 23 and 24 show material constants vs. function of draft (d), and vs. heat-setting temperature (T_f), respectively.

Based on the data comprised in the Tables, the following conclusions can be drawn, concerning the effect of testing temperature, draft and heat-setting temperature:

The effect of testing temperature (T) on the material constants can well be observed in each case and it is, as to the trend of the change and its order of magnitude, unequivocal. Increasing the testing temperature from the lowest value (22 °C) to the uppermost one (100 °C) the material constants have undergone changes as follows:

The elasticity factor E_1 characterizing the momentaneous elastic deformation decreased both in the loading and in the unloading section to its 1/4—1/5.

The decrease of the elasticity factor E_2 characterizing the retarded elastic deformation and of the viscosity factor η_2 varied between 1/4 to 1/30 of their value and the change is always greater in the loading section. The decrease will be checked to a greater extent by the increase of draft and to a lesser extent by the heat-setting temperature.

The material constant of the permanent deformation, the viscosity factor η_1 shows a decrease of 1/2 to 1/60 of its value, which is generally greater in the unloading section. The change will be checked by the higher draft and higher heat-setting temperature.

The processing draft (d) also affects the material constants, according to a marked tendency. When the draft increased, the values of E_1 and η_1 have generally shown — both in the loading and in the unloading section —

Table 2

Four-parameter model analysis of retardation phenomena observed at various temperatures. Specimen characteristics: $d = 3$, $T_f =$ variable

Specimen characteristic	Testing temperature T [°C]	Loading				Unloading			
		$E_1\left[\frac{\text{kp}}{\text{cm}^2}\right] \times 10^4$	$E_2\left[\frac{\text{kp}}{\text{cm}^2}\right] \times 10^4$	$\eta_1\left[\frac{\text{kp·sec}}{\text{cm}^2}\right] \times 10^7$	$\eta_2\left[\frac{\text{kp·sec}}{\text{cm}^2}\right] \times 10^7$	$E_1\left[\frac{\text{kp}}{\text{cm}^2}\right] \times 10^4$	$E_2\left[\frac{\text{kp}}{\text{cm}^2}\right] \times 10^4$	$\eta_1\left[\frac{\text{kp·sec}}{\text{cm}^2}\right] \times 10^7$	$\eta_2\left[\frac{\text{kp·sec}}{\text{cm}^2}\right] \times 10^7$
$d = 3$	22	1.50	4.50	19.6	1.6	1.55	4.74	14.7	2.6
	60	0.73	0.47	4.1	0.2	0.39	0.76	32.4	0.3
	80	0.36	0.26	1.4	0.1	0.31	0.47	0.7	0.2
	100	0.24	0.16	0.9	0.1	0.31	0.48	0.3	0.2
$d = 3$ $T_f = 120$ °C	22	1.27	5.00	2.0	2.6	1.48	3.75	14.7	1.9
	60	0.75	0.71	2.5	0.2	0.48	0.90	8.1	0.4
	80	0.32	0.19	2.1	0.1	0.31	0.40	0.5	0.2
	100	0.30	0.17	1.0	0.1	0.30	0.53	0.3	0.3
$d = 3$ $T_f = 135$ °C	22	1.33	5.14	14.8	1.6	1.64	3.00	1.5	1.6
	60	0.75	0.85	2.4	0.3	0.51	0.62	—5.2	0.2
	80	0.32	0.22	2.0	0.1	0.27	0.46	0.7	0.3
	100	0.30	0.18	1.4	0.1	0.25	0.50	0.4	0.2

Table 3

Four-parameter model analysis of retardation phenomena observed at various temperatures. Specimen characteristics: $d = 3.5$, $T_f =$ variable

Specimen characteristic	Testing temperature T [°C]	Loading				Unloading			
		$E_1\left[\frac{\text{kp}}{\text{cm}^2}\right] \times 10^4$	$E_2\left[\frac{\text{kp}}{\text{cm}^2}\right] \times 10^4$	$\eta_1\left[\frac{\text{kp·sec}}{\text{cm}^2}\right] \times 10^7$	$\eta_2\left[\frac{\text{kp·sec}}{\text{cm}^2}\right] \times 10^7$	$E_1\left[\frac{\text{kp}}{\text{cm}^2}\right] \times 10^4$	$E_2\left[\frac{\text{kp}}{\text{cm}^2}\right] \times 10^4$	$\eta_1\left[\frac{\text{kp·sec}}{\text{cm}^2}\right] \times 10^7$	$\eta_2\left[\frac{\text{kp·sec}}{\text{cm}^2}\right] \times 10^7$
$d = 3.5$	22	1.58	4.74	40.5	1.7	1.44	5.30	32.4	1.8
	60	1.04	0.90	3.6	0.2	0.41	0.85	—1.7	0.3
	80	0.39	0.31	1.5	0.1	0.32	0.54	0.9	0.2
	100	0.37	0.22	1.4	0.1	0.31	0.51	0.6	0.2
$d = 3.5$ $T_f = 120$ °C	22	1.15	4.86	32.4	0.9	1.27	3.34	32.4	1.8
	60	0.78	1.36	3.2	0.1	0.47	0.73	—2.0	0.3
	80	0.56	0.45	2.0	0.3	0.40	0.47	23.2	0.2
	100	0.32	0.23	2.6	0.1	0.36	0.66	0.5	0.2
$d = 3.5$ $T_f = 135$ °C	22	1.07	3.75	29.4	2.1	1.53	2.00	20.3	0.8
	60	0.60	1.25	11.6	0.2	0.42	0.72	1.5	0.3
	80	0.50	0.47	2.1	0.1	0.35	0.47	21.5	0.2
	100	0.31	0.24	2.7	0.1	0.33	0.60	0.5	0.3

Table 4

Four-parameter model analysis of retardation phenomena observed at various temperatures. Specimen characteristics: $d = 4$, T_f = variable

Specimen characteristic	Testing temperature T [°C]	Loading				Unloading			
		$E_1\left[\frac{\text{kp}}{\text{cm}^2}\right] \times 10^4$	$E_2\left[\frac{\text{kp}}{\text{cm}^2}\right] \times 10^4$	$\eta_1\left[\frac{\text{kp·sec}}{\text{cm}^2}\right] \times 10^7$	$\eta_2\left[\frac{\text{kp·sec}}{\text{cm}^2}\right] \times 10^7$	$E_1\left[\frac{\text{kp}}{\text{cm}^2}\right] \times 10^4$	$E_2\left[\frac{\text{kp}}{\text{cm}^2}\right] \times 10^4$	$\eta_1\left[\frac{\text{kp·sec}}{\text{cm}^2}\right] \times 10^7$	$\eta_2\left[\frac{\text{kp·sec}}{\text{cm}^2}\right] \times 10^7$
$d = 4$	22	1.58	5.05	16.2	2.7	1.84	3.75	14.7	1,9
	60	0.94	0.68	5.4	0.3	0.58	0.97	32.4	0.4
	80	0.45	0.42	5.4	0.2	0.38	0.68	2.2	0.3
	100	0.32	0.45	1.8	0.2	0.44	0.49	0.9	0.2
$d = 4$	22	1.43	3.42	24.8	1.1	1.77	3.68	7.9	1.6
$T_f = 120$ °C	60	0.72	1.10	5.8	0.4	0.58	1.28	16.4	0.3
	80	0.43	0.68	5.5	0.2	0.39	0.72	10.8	0.2
	100	0.35	0.40	2.0	0.1	0.30	0.57	1.2	0.2
$d = 4$	22	1.23	3.75	60.0	0.7	1.48	2.31	32.4	1.2
$T_f = 135$ °C	60	0.82	0.95	6.9	0.2	0.44	0.95	−2.2	0.3
	80	0.45	0.82	4.6	0.3	0.39	0.73	−12.5	0.3
	100	0.39	0.78	3.7	0.1	0.37	0.63	23.2	0.2

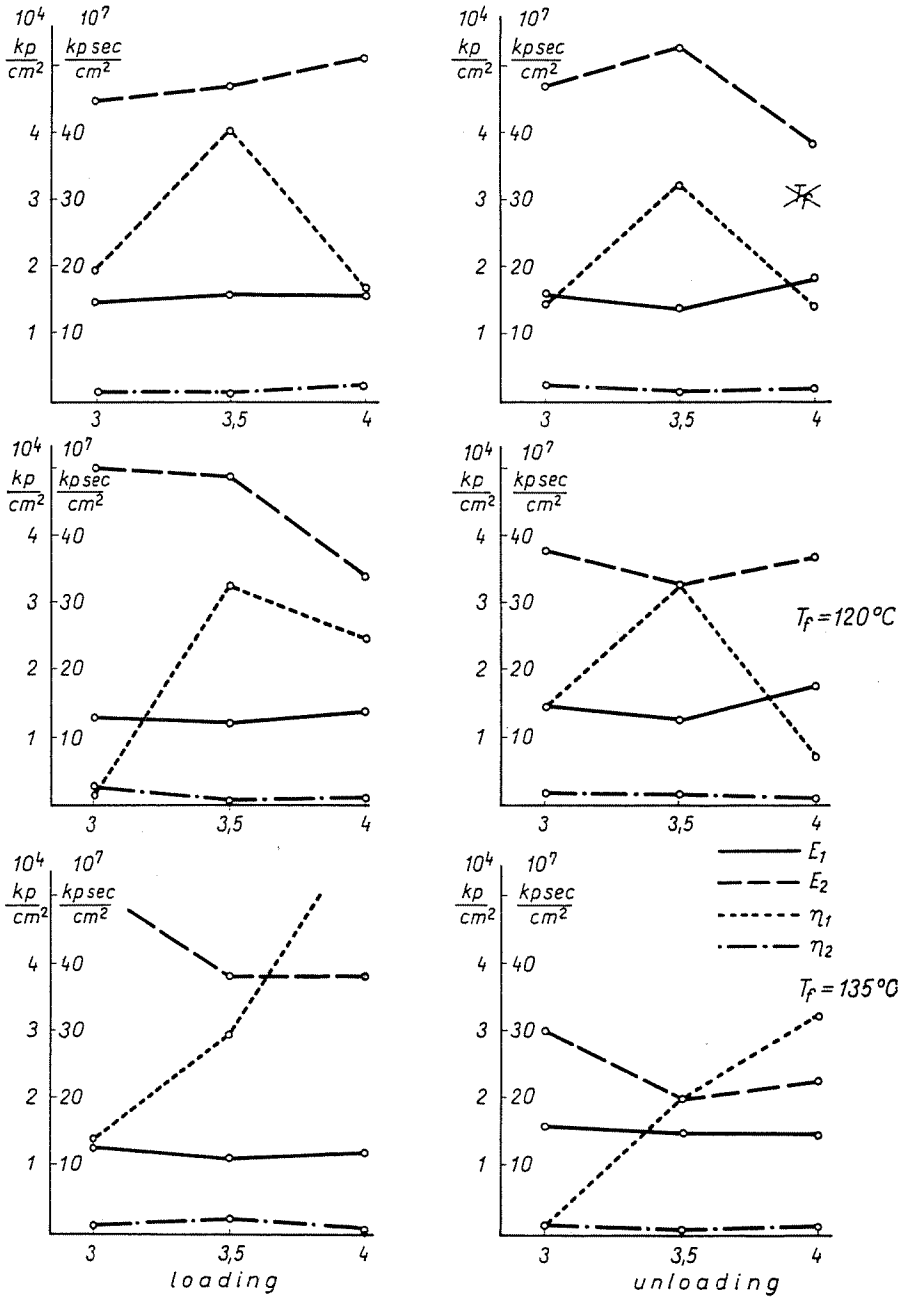

Fig. 23. Material constants determined by means of four-parameter modelling in function of the draft, at various heat-setting temperatures (tests made at 22 °C)

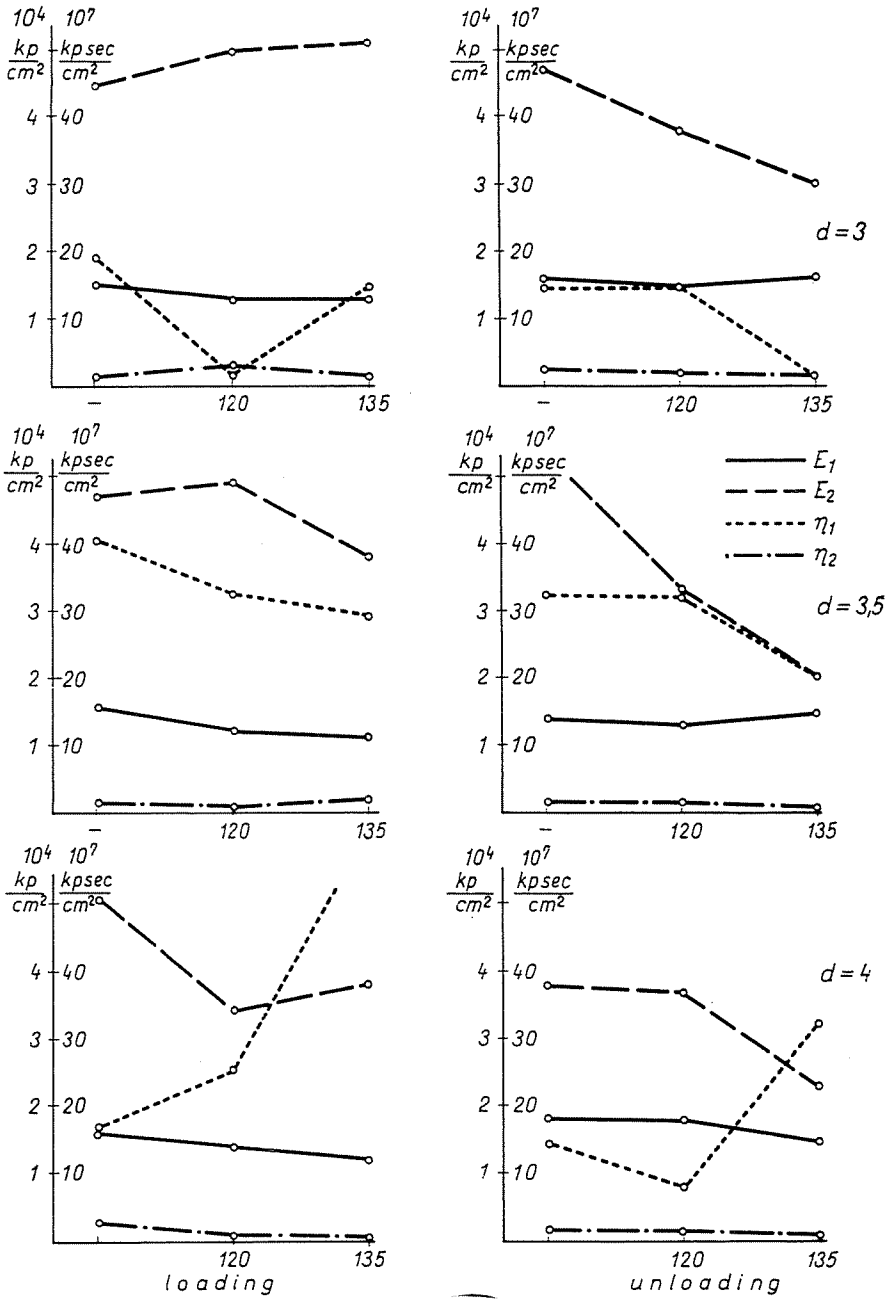

Fig. 24. Material constants determined by means of four-parameter modelling in function of heat-setting, at various drafts (test made at 22 °C)

an increase to a lesser degree, those of E_2 rather decreased. At $d = 3.5$ an optimum could generally be observed for η_1 and several ones for E_2 and η_2.

The effect of the heat-setting temperature (T_f) could, however, be evaluated in a less unequivocal way. It can be surmised that the dispersion of the measurement results (thus the error of the mean value) and the irregularity of processing have in many cases blurred the lesser effect of the heat-setting temperature. At the beginning of heat-setting and at the increase of the setting temperature, respectively, the values of the material constants have either decreased to a lesser extent, or did not show an unequivocal change. (In some cases — especially for η_1 — the temperature 120 °C seemed to be the optimum.)

Our findings connected with the change of the value of the material constants show a good agreement with the results of the analysis given in Chapter 3.

It should finally be remarked that η_1 has proved the most mobile among the material constants and has shown the highest variations, it seems therefore to be the most suitable for detecting *irregularities in the processing* [12].

5. The structure of the fibres tested

In order to follow up the effect of the altered processing parameters (d, T_f), furthermore to explain the differing mechanical characteristics of the specimens, we investigated — and still do it — the inner fibre-structure. Some conclusions of our research work in progress will be discussed now.

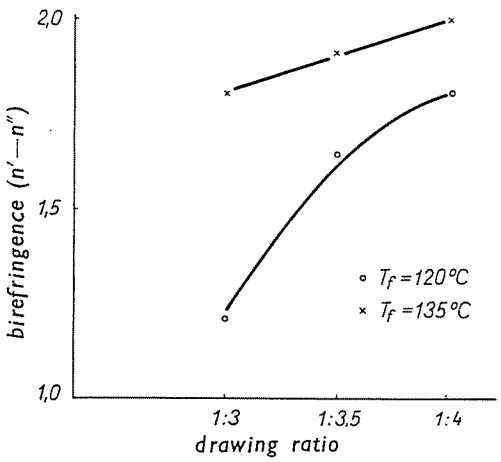

Fig. 25. The change in birefringence of specimens in function of draft at various heat-setting temperatures

The measurements of the birefringence of the fibres have yielded the expected results. Specimens made with a higher draft have shown a higher birefringence (Fig. 25). The obvious explanation is furnished by the higher

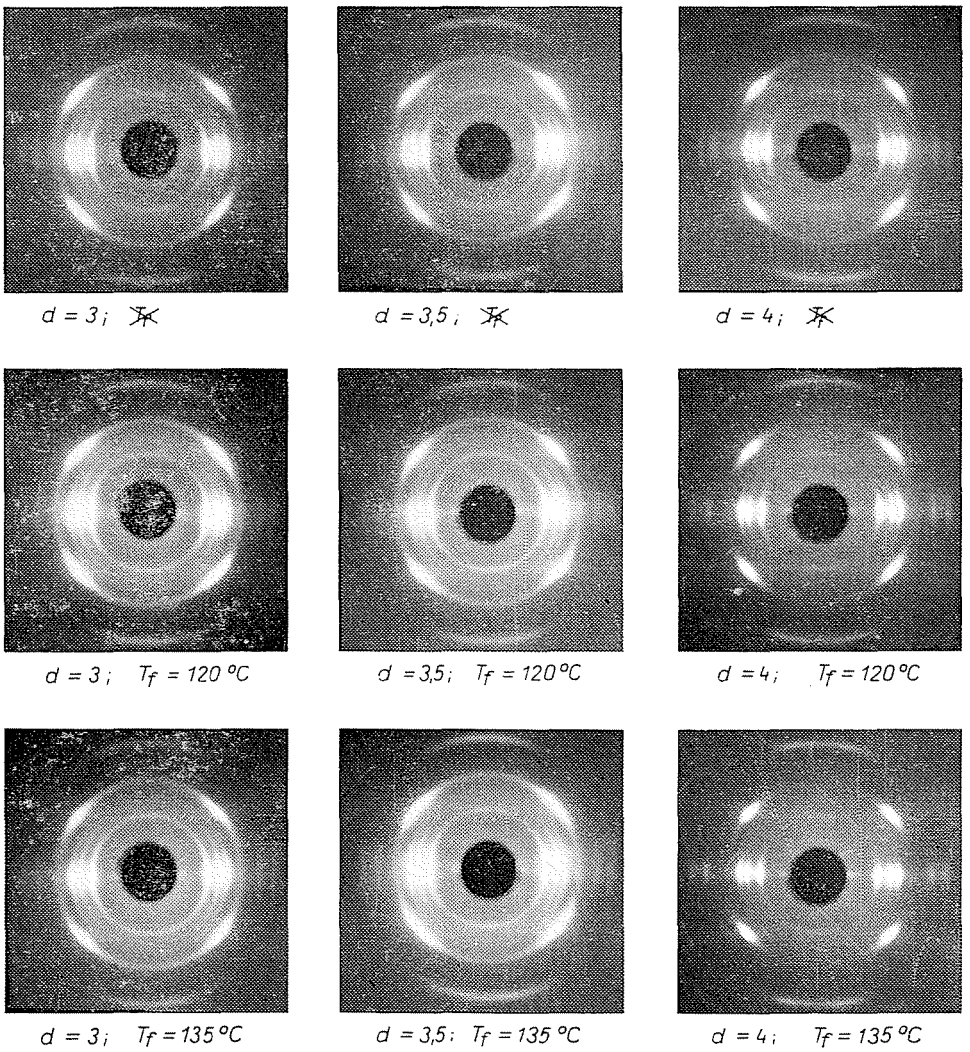

Fig. 26. X-ray diagrams of the specimens

orientation of the molecular structure of fibres manufactured with a higher draft.

In the crystallinity of fibres without heat-treatment and those treated at various temperatures no deviations were found between the limits of the measuring accuracy. The crystallinity of the fibres amounted to $64 \pm 2\%$.

X-ray photos have also been made of the specimens (Fig. 26). The evaluation of the X-ray photos in the first approach has not shown so great difference between the 9 specimens that would explain the difference of the

mechanical characteristics of the various specimens. (We should like to remark, however, that the X-ray diagram of the sample with the characteristics $d = 4$, $T_f = 135\,°C$ also shows the outstanding properties found at this specimen.)

Summarizing the results of our structural tests carried out hitherto, one might suppose that one probable cause of the differences observed in the mechanical properties should be sought in the varying orientation of the amorphous parts. Authors wish to revert to the problem after a more thorough investigation of the inner structure.

6. Conclusions

In our investigations a correlation was sought after between the manufacturing parameters and some of the rheological and structural characteristics. The basic target furthermore was to establish a satisfactory test method. The basic properties of our tests were as follows:

The range of stress employed at our investigations was rather low, not more than 2—3% of the fibre strength. This range was chosen because it is near to the extent of stress occurring in practice. (However we had to take granted the greater dispersion of the test results.)

In course of the investigation of the retardation curves we analysed first of all the section of the recovery from deformation. This section is in close relation to the end-use value, while the formation of the mechanism of the deformation is more of a theoretical concept.

In our work we tried in the first instance to establish relations of tendencies.

Although we did not go very deep in our structural analysis — they still are being carried on — we made several assessments of practical value. Among these we should like to draw attention to the following ones:

The decisive factor from the point of view of the rheological properties and in the first instance, of the deformation recovery, will be the draft applied in the manufacturing process of the fibre. The heat-setting temperature is of a secondary importance, often almost imperceptible. (The role of the heat-setting is especially blurred at higher testing temperatures.)

It is to be noted that in the draft range tested several important material characteristics, such as deformation recovery, shrinking force etc., have shown optimal values at $d = 3.5$ and higher drafts.

The highest relative recovery can be observed at a temperature of 60 °C. At the same time the temperature around 60 °C might be regarded as the elasticity limit of the specimens tested, viz. up to this temperature the fibres still retain their elastic properties.

The material constants — and at the same time the rheological characteristics — are very sensitive to the change of testing and processing conditions; especially mobile are the viscosity factors η. The changes of the parameters of the inner structure are of a lower order of magnitude.

The cause of the inner structure's changes accompanying the modification of the parameters tested is presumably the difference in the orientation of the amorphous part.

Summary

Investigating the effect of manufacturing parameters on the rheological characteristics of polypropylene fibres it was found that the decisive factor is the draft in processing, while the heat-setting temperature plays but a secondary — often almost imperceptible — role. It is to be noted furthermore that in the investigated range of draft it is $d = 3.5$ where several important material characteristics — such as deformation recovery, shrinking force, etc. — show an optimal value. New testing instruments and methods have been applied.

References

1. GELEJI, F.: A hazai polypropilén szálasanyagkutatás eredményei. (The results of Hungarian research of polypropylene fibres.) Magyar Kémikusok Lapja **11**, 571—578 (1966).
2. GELEJI, F.—SZABÓ, K.—HOLLY, Z.—ÓDOR, L.: Ergebnisse der Faserbildung aus Polypropylen und modifiziertem Polypropylen. Abh. der DAW zu Berlin **3**, 29 (1965).
3. BARTHA, Z.—FÜLÖP, I.—NÁDORY, GY.: Einige Probleme der rheologischen Untersuchung syntetischer Kordzwirne. III. Internationales Symposium für Gummi. Gottwaldow, 1971.
4. FÜLÖP, I.—NÁDORY, GY.: Szóráselemzés alkalmazása poliamid kordcérnák reológiai tulajdonságainak összehasonlító elemzésénél. (The application of analysis of variance in the comparative analysis of the rheological properties of cords.) Magyar Textiltechnika **11**, 613—620 (1970).
5. GELEJI, F.—HOLLY, S.: Szerves pigmentek hatása polipropilén szál hő- és fénystabilitására. (The effect of organic pigments on the heat- and light-stability of polypropylene fibres.) Magyar Kémikusok Lapja **9**, 477—482 (1968).
6. KÓCZY, L.: Mesterséges szálasanyagok. (Nagymolekulájú polimerek fiziko-mechanikája.) (Manmade fibres — Physico-mechanics of macromolecular polymers.) Tankönyvkiadó, Budapest, 1965.
7. GELEJI, F.: On the modification of properties of polypropylene fibres. Chemické Vlakna **18**, 114 (1968).
8. STUART, H. A.: Die Physik der Hochpolymeren. 4. Bd. Berlin—Göttingen—Heidelberg, Springer, 1956.
9. MCKELVEY, I. M.: Polimerek feldolgozása. (The processing of polymers.) Budapest, Műszaki Könyvkiadó, 1966.
10. KÓCZY, L.: Rheological model for the analysis of the relaxation of visco-elastic materials. Moscow, CNIITEI legrom, 48—50, 1967.
11. KÓCZY, L.: Verfahren und Gerät zum Modellieren und Analysieren von rheologischen Kurven. Jubilarische wissenschaftliche Tagung, 9. Juni 1969, Budapest. Der Textiltechnische und Wissenschaftliche Verein Ungarns. 83—92
12. KÓCZY L.: Controle de l'irrégularité des filaments et des produits de filature. Lecture delivered at the Association Nationale de la Recherche Technique, Paris, 1971.
13. FÜLÖP, I.: Prelucrarea fibrelor sintetice (Prelucrarea mecanică). IDT. București, 1959.

Dr. László KÓCZY
Dr. István FÜLÖP
Dr. Frigyes GELEJI
Budapest, XI., Sztoczek u. 2—4. Hungary